



CHALMERS
UNIVERSITY OF TECHNOLOGY

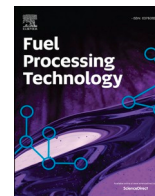
Chemical-looping combustion in packed-fluidized beds: Experiments with random packings in bubbling bed

Downloaded from: <https://research.chalmers.se>, 2026-04-05 04:53 UTC

Citation for the original published paper (version of record):

Nemati, N., Rydén, M. (2021). Chemical-looping combustion in packed-fluidized beds: Experiments with random packings in bubbling bed. *Fuel Processing Technology*, 222. <http://dx.doi.org/10.1016/j.fuproc.2021.106978>

N.B. When citing this work, cite the original published paper.



Chemical-looping combustion in packed-fluidized beds: Experiments with random packings in bubbling bed

Nasrin Nemati^{*}, Magnus Rydén

Division of Energy Technology, Department of Space, Earth and Environment, Chalmers University of Technology, Göteborg, Sweden

ARTICLE INFO

Keywords:

Bubbling fluidized bed
Packed-fluidized bed
Confined fluidization
Ilmenite
Oxygen carrier
Chemical-Looping Combustion

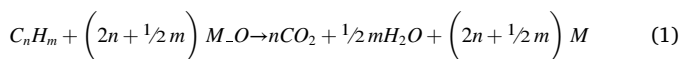
ABSTRACT

Chemical-looping combustion (CLC) in packed-fluidized bed reactor was investigated. Experiments were carried out in a cylindrical laboratory-scale bubbling fluidized-bed reactor with an inner diameter of 78 mm and a height of 1.27 m. Ilmenite concentrate particles in the size range 90–212 μm was used as oxygen carrying fluidizing solid. Two different types of random packings were used: aluminum silicate balls (ASB) with a diameter of 12.7 mm and bulk density of 1439 kg/m^3 and 25 mm stainless steel thread saddles (RMSR) with bulk density of 204 kg/m^3 . The superficial gas velocity was 0.3 m/s. The fuels were CO and CH_4 . The bed temperature was 840 °C for CO and 940 °C for CH_4 . The height of the packed bed was kept constant at 1 m. The fluidized oxygen carrier bed height was varied from 2 cm to 40 cm. Results showed that fuel conversion in packed-fluidized beds is highly dependent on oxygen carrier bed height and the nature of the packing. Packed-fluidized beds with RMSR packing resulted in a significant improvement in fuel conversion, compared to a bubbling bed with no packing. With 30–40 cm bed height, CO conversion was $\approx 99.5\%$ with RMSR packing and 91–96% without packing. The corresponding numbers for CH_4 were $\approx 84\%$ and $\approx 78\%$. Further, the RMSR packing has very high void factor (0.96). Thus, it should have limited effects on particle inventory, pressure drop and throughput. The most likely mechanism for improved fuel conversion is improved gas-solid mass transfer due to be reduced bubble size. The ASB packing has low void factor (0.43) and provided mixed results with respect to fuel conversion.

1. Introduction

Chemical-Looping-Combustion (CLC) is a promising technology for generation of heat and power with inherent CO_2 capture. The chemical-looping concept also have other potentially important applications such as combustion, gasification, reforming, and hydrogen production [1–6]. CLC utilize solid metal oxide particles and a setup with two interconnected reactions, typically referred to as the Air Reactor (AR) and Fuel Reactor (FR), see Fig. 1.

In the fuel reactor, the oxygen carrier particles are reduced by the fuel (C_nH_m), which in turn is oxidized to CO_2 and H_2O . In the air reactor, the particles are oxidized with O_2 from air. The reactor temperature is typically in the range 800–1000 °C. An example of the reactions in each reactor vessel and for the whole system can be found in reactions (1–2) below, where M_O represents the oxidized oxygen carrier and M the reduced oxygen carrier.



The main advantage with CLC is that it prevents dilution of flue gases with air and eliminates the need for a separate and costly gas separation step after combustion [7–10]. The reactors in the CLC process can be designed using different principles, such as bubbling fluidized bed, circulating fluidized bed, fast fluidized bed, moving bed or fixed bed [11–15]. Among the alternatives, two interconnected fluidized bed reactors presents advantages such as good temperature control and steady flow of oxygen carrier particles between the air reactor and fuel reactor [1]. One challenging issue with fluidized bed reactors is the potential for reduced gas-solid mass transfer at high superficial gas velocities when deep beds are used, due to bubble growth. Large bubbles result in reduced contact between gases and solids which is necessary to achieve high fuel conversion. It could also lead to other undesirable fluidization phenomena such as slugging.

The idea to apply random packings in fluidized bed reactors to prevent bubble growth in chemical-looping combustion has recently been suggested [16]. The concept of using random packings in fluidized beds is referred to as packed-fluidized bed or confined fluidization. The effect

^{*} Corresponding author.

E-mail address: nasrinn@chalmers.se (N. Nemati).

Nomenclature

i	component i (–)
m	momentary mass of the oxygen carrier (kg)
M_o	molar mass of oxygen (kg/mol)
m_{ox}	mass of oxygen carrier in its fully oxidized form (kg)
n^*	total molar flow rate at the reactor outlet (mol/s)
n_i^*	molar flow rate of component i (mol/s)
t	time (s)
x	conversion of oxygen carrier (–)
y_i	outlet volume fraction of gas component i (–)
γ	fuel gas conversion (–)
ω	degree of oxygen carrier reduction (–)

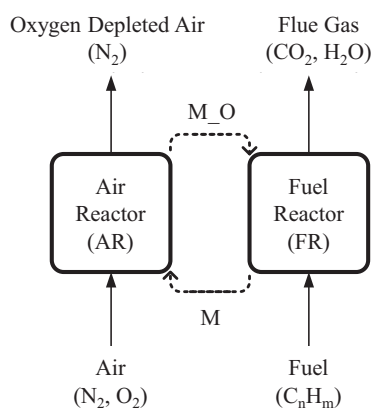


Fig. 1. Schematic description of Chemical-Looping Combustion (CLC).

of packings on fluidization was first investigated by Gabor and Mecham [17] and Sutherland et al. [18], who investigated the effect of spherical packings on hydrodynamics and heat transfer rates in fluidized beds. They documented fundamental fluidization properties and observed that a combination of packed beds and fluidized beds can improve the heat transfer rate. A few studies on packed-fluidized beds have been done afterwards about topics such as catalytic reactions [19–22] and hydrodynamic properties such as minimum fluidization properties and pressure drop [23–26]. However, there is still a lack of basic research and understanding of this field.

Recently, Aronsson et al. [16] successfully applied spherical packings in CLC batch experiments and found improved fuel conversion rates compared to a conventional bubbling fluidized bed. However, there are no studies on other forms of packings and their effect on fuel conversion in this field of research.

1.1. Aim of this study

The aim of the present work is to investigate the use of non-spherical random packing material RMSR 25–3 packings in CLC batch experiments. This family of packings is deemed interesting for this application since it has a void factor $> 95\%$. Therefore, it has negligible impact on oxygen carrier inventory in a given reactor and could be expected to have limited impact also on pressure drop and solid flux. The results are benchmarked against spherical packings (ASB) and bubbling bed without packings.

2. Method

2.1. Bed material and packings

In this work, ilmenite concentrate was used as fluidizing solid in the reactor. Ilmenite mineral is an ore consisting of iron and titanium oxides ($FeTiO_3$, Fe_2TiO_5 , Fe_2O_3 , TiO_2 , Fe_3O_4) and various impurities. Ilmenite concentrate has been ground and physically beneficiated to increase the content of iron and titanium oxides. Ilmenite as oxygen carrier in chemical-looping-combustion (CLC) has been thoroughly investigated in the literature and been shown to be an attractive and affordable bed material for this process [27–30]. One problematic aspect when using ilmenite in experiments is that the material tends to change physical properties during operation. Ilmenite particles that has been subject to repeated oxidation and reduction typically has lower density compared to the fresh particles, and displays improved reactivity with fuel and increased porosity [30]. This behavior can create problems when analyzing data generated during experiments. However, by using ilmenite that has been activated over numerous redox cycles the risk for such problematic behavior can be minimized [31]. Thus, in this study, ilmenite particles that previously had been utilized as bed material in a continuous CLC pilot reactor was used. The batch of particles was generated in the campaign by Moldenhauer et al. [32] and have previously also been used in other experimental work [16,33]. The measured bulk density of particles was 1633 kg/m^3 , when calculated by pouring ilmenite particles into a container with a known volume, measuring its change in mass and dividing it by its volume. The ilmenite particles were sieved to the size range $90\text{--}212 \mu\text{m}$. The average diameter of particles was $178.9 \mu\text{m}$.

Two different types of packings were used. The first was aluminum silicate balls (ASB) with a diameter of 12.7 mm , a void factor of 0.43 and bulk density of 1439 kg/m^3 . The second was an evolved packing supplied by RVT process equipment GmbH, namely 25 mm stainless steel thread saddle RMSR (Rauschert Metal Saddle Rings). It has a surface of $235 \text{ m}^2/\text{m}^3$, a void factor of 0.96 and a bulk density of 204 kg/m^3 . Due to excellent mechanical strength and mass transfer efficiency of RMSR saddles, their typical applications are in H_2S absorption and stripping towers, quench towers, steam stripping, distillation, CO_2 absorption and stripping and etc. Fig. 2 shows pictures of the packings used in this study and Table 1 describes their main properties.

2.2. Gases

Investigated fuel gases were carbon monoxide (CO) and methane (CH_4). Nitrogen (N_2) was applied as the inert gas and air was used in the oxidation step as the oxidizing gas. The flow rates of gases during operation are specified in Table 2.

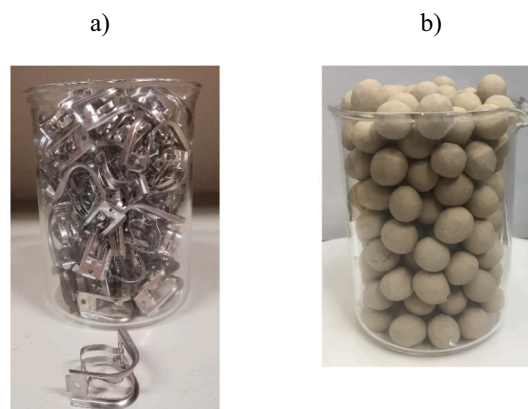


Fig. 2. Pictures of packings used in this study: a) stainless steel thread saddle (RMSR), b) aluminum silicate balls (ASB).

Table 1
The characteristics of packings.

Packing	Material	Void factor of packing (-)	Bulk density (kg/m ³)	Nominal size (mm)
RMSR	Stainless steel	0.96	204	25
ASB	Aluminum silicate	0.43	1439	12.7

Table 2
The flow rate of gases during the batch CLC process.

Process	Oxidation	Inert	Reduction with CO		Reduction with CH ₄	
Gas	Air	N ₂	CO	N ₂	CH ₄	N ₂
Flow rate (L _n /min)	21	10	15	6	10	9

2.3. Experimental setup

Fig. 3 shows the reactor system used in this work. Experiments were conducted in a cylindrical laboratory-scale reactor made of high temperature 253 MA steel. The reactor had an inner diameter of 78 mm and a height of 1.27 m. The fuel gas, N₂ and air was fed into the system by Bronkhorst El-Flow Prestige FG-201CS mass flow controllers (MFC), with less than 0.2% deviation. The gases entered the reactor via the windbox. A gas distribution plate with 61 circular 0.6 mm holes and a thickness of 5 mm was located at the top of the windbox. A small gas flow was applied also during down time, to prevent particles smaller than the holes of the distributor plate to fall into the windbox. The reactor was located inside an electric furnace, allowing it to reach desirable temperature levels. Since the windbox was located inside the furnace, the fuel, air and inert gas were pre-heated to temperatures close to bed temperature before entering the reactor. The hot gas exiting the reactor was collected by a ventilation hood located above the reactor exit.

Horizontal gas sampling tubes were connected to the bed through the front wall of the reactor to collect and analyze gas compositions. Only one was in use at each given time, while the rest were plugged. Also, several pipes, inclined at 45°, were connected to the system through the back side of the reactor at the same measurement point as sampling tubes to collect the temperature and pressure signal data. Table 3 illustrates vertical positions of the measurement points relative to distributor plate. To avoid condensation in the sampling gas, a heated PTFE tube was applied to the chosen sampling tube, so that the gas

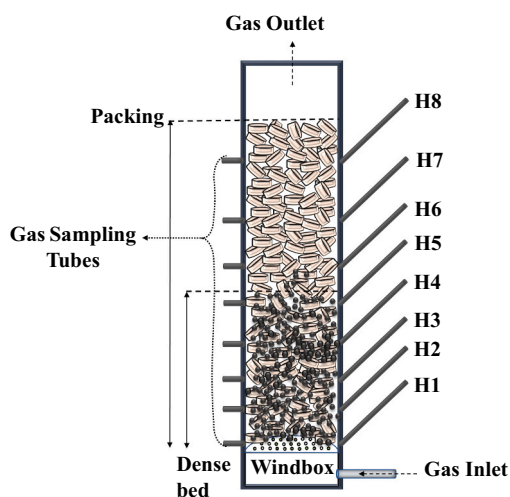


Fig. 3. Schematic illustration of the experimental reactor system and gas sampling tubes.

Table 3
Vertical position of measurement points relative to the distributor plate.

Position	Height (cm)	Measured data
Windbox	-	Temperature and Pressure
1	3.65	Temperature and Pressure
2	8.88	Temperature and Pressure
3	13.65	Temperature and Pressure
4	15.65	Temperature and Pressure
5	31.65	Temperature and Pressure
6	47.65	Temperature and Pressure
7	63.65	Temperature and Pressure
8	79.65	Temperature and Pressure

temperature was kept at approximately 190 °C. The gas analyzing instrument was a SICK GMS810, which was equipped with a thermal conductivity sensor for H₂, nondispersive infrared sensors for CH₄, CO and CO₂, and a paramagnetic sensor for O₂. The flow rate to the gas analyzing instrument was 2 L_n/min. Gas samples were collected from sampling point 6 (47.65 cm above distributor plate) for bed heights up to 10 cm and from sampling point 7 (63.65 cm above distributor plate) for bed heights in the range of 15–40 cm.

2.4. Experimental procedure

For packed-fluidized bed experiments, the reactor was first filled with packings up to 1 m height. Then, ilmenite particle was added gradually from a minimum bed height of 2 cm up to maximum bed height of 40 cm. For each bed height a number of reduction and oxidation cycles were conducted, during which pressure, temperature and outlet gas concentration data were recorded for analysis. During heat up, the bed was fluidized with 21 L_n/min air. The reactor set temperature was 840 °C for CO experiments and 940 °C for CH₄ experiments. The reason for using different temperatures for the two fuels is the well-established difference in the reaction rate in CLC for these two gases, when using ilmenite as oxygen carrier. Thus, since the aim of the study was to examine the impact of packing materials, rather than the impact of temperature on the reactivity of ilmenite with fuel gases, the temperature levels were chosen so that high but not complete fuel conversion could be expected. By doing so, any improvement when using packings could be seen clearly. After stabilization of bed temperature on the chosen level, the flow was switched to inert N₂, followed by fuel once the reactor was flushed from oxygen. The flow rates are reported in Table 2 above. Fuel was fed to the reactor for a sufficiency long time period, so that a mass-based conversion of oxygen carrier (X) of about 0.8 wt% was achieved. Consequently, the reduction period varied between 3 s and 120 s based on the amount of ilmenite in the bed, see Table 4 below.

After the reduction period, fuel feeding was changed to N₂ with 10 L_n/min flow rate for 300 s to ensure that the reactor was completely purged from fuel. Finally, air was introduced into the bed with 21 L_n/min flow rate and oxidation of ilmenite proceeded until the O₂ concentration in the bed reached its initial value. Each set of experimental parameters was repeated at least two times to ensure that the gathered data were stable and predictable. Once finished, more bed material was added to reach the next experimental bed height. Then, the procedure explained above was repeated for the new bed height and so on. Also, a set of experiments were done without packings to have as reference.

A summary of the experiments performed are gathered in Table 4. The reason for the slightly different bed heights used for RMSR packing is that the bed mass added was based on a provided void factor which, when checked, was proven to be incorrect. Thus, the bed heights were recalculated after new measurements of void factor. This should not have major implications for conclusions, as will be shown below.

Table 4
Performed experimental data. Packing height was fixed at 1 m in beds with packing.

No.	Packing	Fuel	Settled bed height (cm)	Ilmenite mass in bed (kg)	Time of reduction (s)
1	–	CO	2	0.15	6
2	–	CO	3	0.23	9
3	–	CO	5	0.39	15
4	–	CO	10	0.78	30
5	–	CO	15	1.17	45
6	–	CO	20	1.56	60
7	–	CO	30	2.34	90
8	–	CO	40	3.12	120
9	RMSR-saddle	CO	1.8	0.15	6
10	RMSR-saddle	CO	2.7	0.22	9
11	RMSR-saddle	CO	4.4	0.37	15
12	RMSR-saddle	CO	8.8	0.75	30
13	RMSR-saddle	CO	13.3	1.12	45
14	RMSR-saddle	CO	17.7	1.50	60
15	RMSR-saddle	CO	26.6	2.25	90
16	RMSR-saddle	CO	35.4	2.99	120
17	ASB	CO	2	0.07	3
18	ASB	CO	3	0.10	5
19	ASB	CO	5	0.17	8
20	ASB	CO	10	0.33	15
21	ASB	CO	15	0.50	23
22	ASB	CO	20	0.67	30
23	ASB	CO	30	1.01	45
24	ASB	CO	40	1.34	60
25	–	CH ₄	2	0.15	3
26	–	CH ₄	3	0.23	5
27	–	CH ₄	5	0.39	8
28	–	CH ₄	10	0.78	15
29	–	CH ₄	15	1.17	23
30	–	CH ₄	20	1.56	30
31	–	CH ₄	30	2.34	45
32	–	CH ₄	40	3.12	60
33	RMSR-saddle	CH ₄	1.8	0.15	3
34	RMSR-saddle	CH ₄	2.7	0.22	5
35	RMSR-saddle	CH ₄	4.4	0.37	8
36	RMSR-saddle	CH ₄	8.8	0.75	15
37	RMSR-saddle	CH ₄	13.3	1.12	23
38	RMSR-saddle	CH ₄	17.7	1.50	30
39	RMSR-saddle	CH ₄	26.6	2.25	45
40	RMSR-saddle	CH ₄	35.4	2.99	60
41	ASB	CH ₄	2	0.07	1
42	ASB	CH ₄	3	0.10	2
43	ASB	CH ₄	5	0.17	3
44	ASB	CH ₄	10	0.33	6
45	ASB	CH ₄	15	0.50	9
46	ASB	CH ₄	20	0.67	12
47	ASB	CH ₄	30	1.01	18
48	ASB	CH ₄	40	1.34	24

2.5. Data evaluation

In this study, CO and CH₄ was used as fuel, for which eq. (1) can be written as eqs. (3) and (4) respectively:



The conversion of fuel gas to CO₂ (γ) is defined in expression (5) for CO and (6) for CH₄:

$$\gamma_{CO} = 1 - \frac{n^*_{CO,out}}{n^*_{CO,out} + n^*_{CO_2,out}} = \frac{n^*_{CO_2,out}}{n^*_{CO,out} + n^*_{CO_2,out}} \tag{5}$$

$$\gamma_{CH_4} = 1 - \frac{n^*_{CH_4,out} + n^*_{CO,out}}{n^*_{CH_4,out} + n^*_{CO_2,out} + n^*_{CO,out}} \tag{6}$$

where n_i^{*} is the molar flow rate of component i.

The oxygen carrier conversion (X) is defined in expression (7):

$$X = 1 - \frac{m}{m_{ox}} \tag{7}$$

where, m is the momentary mass of the oxygen carrier and m_{ox} is the mass of oxygen carrier when fully oxidized.

The momentary oxygen carrier conversion is calculated according to eq. (8) for CO and eq. (9) for CH₄.

$$X_i = X_{i-1} + \int_{t-1}^t \frac{n^* M_O}{m_{ox}} (y_{CO_2}) dt \tag{8}$$

$$X_i = X_{i-1} + \int_{t-1}^t \frac{n^* M_O}{m_{ox}} (4y_{CO_2} + 3y_{CO} - y_{H_2}) dt \tag{9}$$

where, M_o is the molar mass of oxygen, n^{*} is the total molar flow rate at the reactor outlet and y_i is the outlet volume fraction of gas component i.

In CLC, it is common that fuel conversion varies slightly with the degree of oxidation of the oxygen carrier. Typically, a fully oxidized oxygen carrier provides higher fuel conversion than a reduced oxygen carrier. In this paper, fuel conversion data are reported predominantly as the average values for γ_{CO} and γ_{CH₄} for ω ranging from 0.999 to 0.992. Data for ω > 0.999 are not included since the immediate transient period following the switching of gases are difficult to interpret for the reactor setup used. Reduction then proceeds to ω = 0.992 or 0.8 wt%, which is considered as a reasonable degree of reduction for ilmenite in future practical applications.

3. Results

3.1. Average fuel conversion as function of bed height

Average fuel conversion for ω = 0.992–0.999 as function of bed height is depicted in Figs. 4-5.

Fig. 4-5 shows that in general deeper beds provide improved fuel

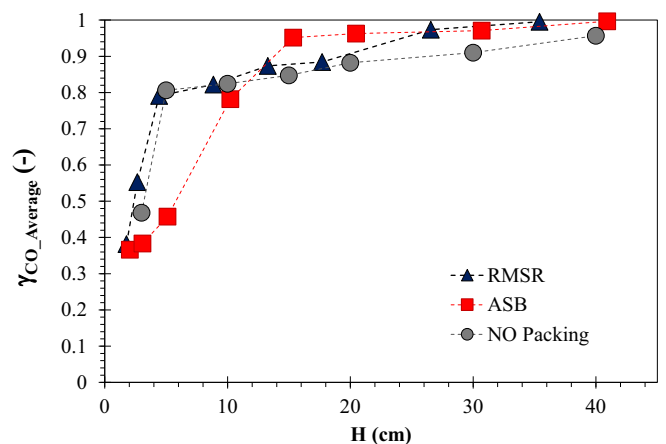


Fig. 4. Average CO conversion (γ_{CO_Average}) as function of bed height H at 840 °C.

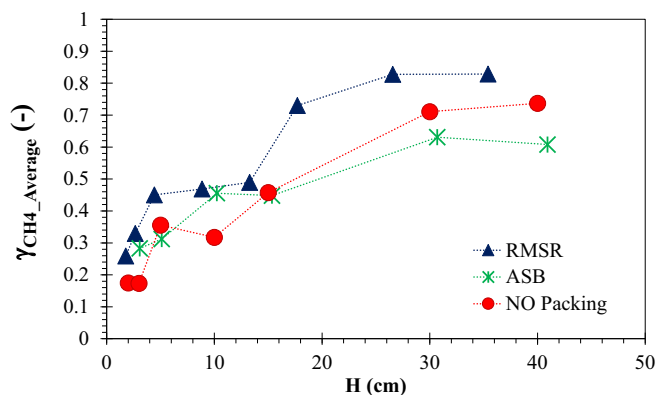


Fig. 5. Average CH₄ conversion ($\gamma_{CH_4_Average}$) as function of bed height H at 940 °C.

conversion. This is expected since a deep bed allows for longer residence time and increased opportunities for the fuel to meet the oxygen carrier. With bed depths lower than approximately 15 cm the effect of adding packings is not clear, but there seems to be an improvement in CH₄ conversion with RMSR. It shall be pointed out that the packing materials used has the nominal dimensions of 12.7 mm and 25 mm. For low bed heights this means that the packing depth is only a few stacked layers of packing, which may be insufficient to achieve an even flow profile. Also bubble size could be expected to be small with low bed height, leaving limited space for improvement. See section 4 below for further discussion.

For beds deeper than 15 cm, CO conversion is much improved compared to beds with no packing at the same bed height. This observation agrees well with results presented by Aronsson et al. [16] who investigated semi spherical expanded clay aggregates and ASBs as packings for syngas and CO at 915 °C. It was observed that fuel conversion increased for both spherical packings, compared to a bed with no packing under the experimental conditions used, i.e. bed height range of 5–25 cm and superficial gas velocity of 0.23 m/s. In a packed bed with a depth of 35 cm there is essentially full conversion of CO already at 840 °C.

The impact of packings on CH₄ conversion was less straightforward. RMSR packing resulted in a significant improvement, while ASB packing resulted in reduced performance, compared to the reference case without packing. Possible explanations will be discussed in section 4 below.

3.2. Average fuel conversion as function of bed mass

Average fuel conversion for $\omega = 0.992$ – 0.999 as function of bed mass is depicted in Figs. 6–7. These figures are related to Fig. 4–5 via the void factor of the packings, meaning that the bed mass for a certain bed height when using ASB packing is much lower than for the RMSR packing.

In Fig. 6–7, it can be seen that addition of packings can reduce the need for oxygen carrier particles significantly. For example, Fig. 6 shows that in order to achieve 97% CO conversion in beds with no packings, more than 3.1 kg ilmenite is needed. In packed-fluidized beds containing RMSR packings, the amount will decrease to 2 kg and for ASB packings it will decrease to around 1 kg. Fig. 7 shows that for packed-fluidized beds containing RMSR packings, CH₄ conversion reaches >70% with 1.3 kg oxygen carrier, while more than 3 kg is needed in a bubbling bed with no packings.

3.3. Average fuel conversion as function of pressure drop

Fig. 8–9 show the effect of packings on fuel conversion as function of

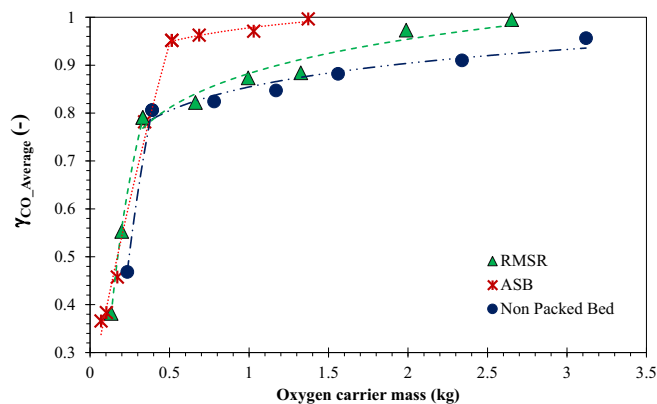


Fig. 6. Average CO conversion ($\gamma_{CO_Average}$) as function of fluidizing solid mass at 840 °C.

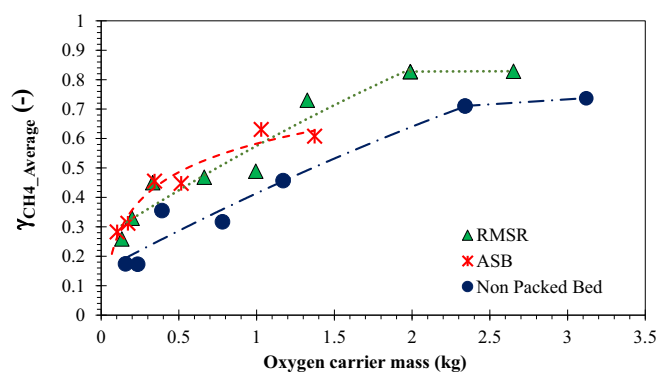


Fig. 7. Average CH₄ conversion ($\gamma_{CH_4_Average}$) as function of fluidizing solid mass at 940 °C.

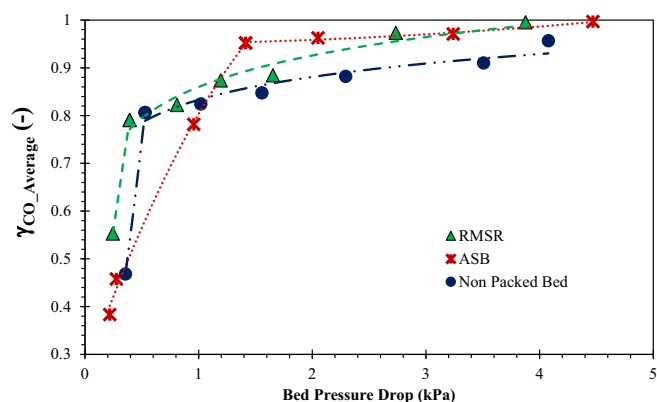


Fig. 8. Average CO conversion ($\gamma_{CO_Average}$) as function of pressure drop over the bed at 840 °C.

pressure drop.

Fig. 8 follow the expected pattern, with significant improvements in fuel conversion for given pressure drop for both ASB and RMSR for the cases which corresponds to deeper bed heights than 15 cm. For example, Fig. 8 shows that for 97% CO conversion, the pressure drop with RMSR packing is around 2.6 kPa while it increases to 3.2 kPa and more than 4.1 kPa for ASB and non-packed beds respectively. This trend agrees well with literature that correlates pressure drop with fluidizing solids and packing mass [16,34]. The improvement for ASB is less dramatic than for the case looking at mass in Fig. 6. In Fig. 9 it can be seen that the

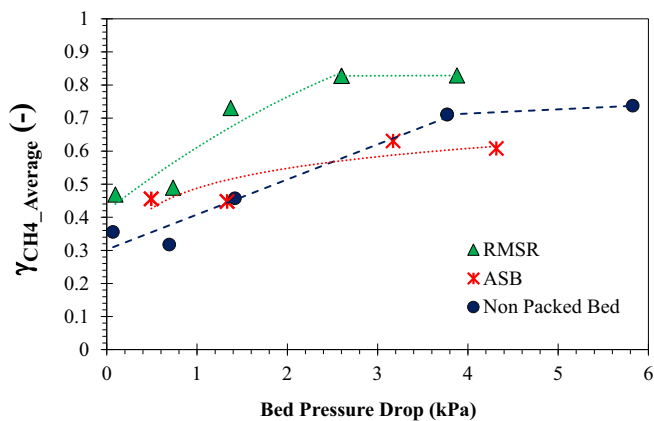


Fig. 9. Average CH₄ conversion ($\gamma_{CH_4_Average}$) as function of pressure drop over the bed at 940 °C.

pressure drop for a given conversion rate of CH₄ is much lower in the RMSR packed-fluidized bed, compared to the alternatives.

3.4. Fuel conversion as function of oxygen carrier conversion in deeper bed

A comparison between fuel conversion γ for beds 26–40 cm as function of ilmenite conversion X is shown in Fig. 10-11.

It can be observed from Fig. 10 that the while the degree of reduction of the oxygen carrier influences the results, relatively stable fuel conversion is achieved over the whole reduction period.

4. Discussion

The results presented in Figs. 4-11 show that the addition of packings to a bubbling fluidized bed, under most circumstances, improves fuel conversion. In many instances the improvement is very significant. The effect is limited or non-existent at low bed heights but becomes more noticeable in deeper beds. This observation is believed to be due to bubble formation and bubble growth in the bed. In a shallow bed the bubbles are small in size and the effect of the packing on gas-solid mass transfer could be expected to be low. But by increasing the bed height, bubbles will have the chance to coalesce and grow in the bed with no packings. Thus, the surface area between bubbles and oxygen carrier will decrease. At higher bed heights, Packed- fluidized beds can improve the average conversion of fuel gas to values higher than non-packed beds by preventing bubble growth and by breaking down bigger bubbles into smaller ones.

Aronsson et al. [16] who investigated semi spherical expanded clay

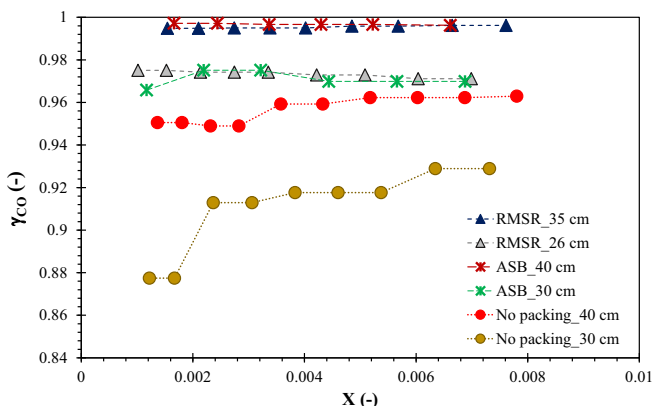


Fig. 10. CO conversion γ_{CO} as function of X at 840 °C.

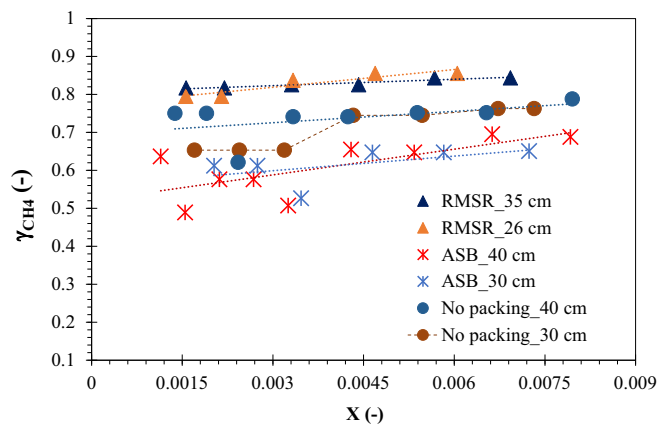


Fig. 11. CH₄ conversion γ_{CH_4} as function of X at 940 °C.

aggregates and ASB as packings for CLC experiments suggested that the increases in fuel conversion is due to an improvement of the gas-solid mass transfer through the inhibition of bubble growth. The mechanism would be that the packings becomes a physical constraint on bubble size. Aronsson et al. [26] have also shown increased mass transfer rate of water vapor in humid air to fluidized silica gel particles during experiments performed in a cold-flow model.

It is important to point out that the gas-solid mass transfer is only one factor influencing fuel conversion in CLC. Reaction kinetics between the fuel and oxygen carrier is another very important factor, which differs greatly for different combinations and process parameters. Packings will affect the fuel conversion only if mass transfer is a significant bottleneck, which for current experiments seems to be bed heights greater than 15 cm.

As outlined in Table 1, RMSR has a void factor of 0.96. So, in a bubbling fluidized bed with RMSR packing the fluidized particles and gas occupy 96% of the space. While not explicitly examined in this paper, this sort of packing is not expected to have huge negative impact on most other key parameters. Previous studies have shown very limited impact of RMSR packing on factors such as heat transfer and particle segregation [35,36]. However, the results presented in this paper suggests that RMSR packing retains the ability to hinder bubble growth and improve gas-solid mass transfer. While it would not be uncomplicated to apply packings in solid fuel CLC, this could be an interesting approach to improve the overall performance of the CLC fuel reactor without the need for the use of exotic and expensive oxygen carriers. For gaseous fuel application the design of a packed-fluidized bed reactor could be rather straightforward. For solid fuel applications more elaborate designs that differs from conventional solid fuel boilers might be needed. Notably, top feeding of solid fuels seems unlikely to be capable of taking full advantage of the concept.

In Table 1 it can also be seen that ASB has a void factor of 0.43, meaning that in a bubbling fluidized bed with ASB packing the fluidized particles and gas would occupy only 43% of the space. This is expected to have very significant impact on factors such as solids throughflow, as have been shown by Aronsson et al. [26]. Also, ASB packings is expected to intensify tendencies towards channeling, which could result in reduced mass transfer and increase vertical segregation of particles. Such tendencies have been observed during cold-flow experiments with ASB packing, but as of this moment this phenomenon has not been studied in detail. Similar tendencies have not been seen for RMSR packings. Increased tendencies towards channeling could be an explanation for the relatively poor performance with ASB for experiments with CH₄. Note that the actual gas velocity will be up to 90% higher for the CH₄ experiments than for the CO experiments, due to the volume expansion during CH₄ conversion and the higher temperature used. This could have a profound effect on channeling.

5. Conclusion

The effect of adding two different kinds of random packings to a bubbling fluidized bed during CLC experiments was examined. The oxygen carrier was ilmenite concentrate. The packings were 12.7 mm ASB and 25 mm RMSR. Reduction was performed with two fuels, CO at 840 °C and CH₄ at 940 °C. Oxidation was performed with air. The following conclusions could be drawn:

- At bed heights lower than 15 cm, beds with RMSR and ASB packings had roughly the same fuel conversion as an ordinary bubbling bed without packings.
- For bed heights 15–40 cm, γ_{CO} improved drastically when RMSR or ASB packing were used, compared to the corresponding case with no packing. CO conversion >99.5% was achieved with bed height above 30 cm for packed-fluidized bed, while the unpacked bed had γ_{CO} of 91–96%. This can be considered as a dramatic improvement. It is believed that it has to do with improved gas-solid mass transfer due to hampering of bubble growth.
- For bed heights 15–40 cm, also γ_{CH_4} improved greatly when RMSR packing were used, compared to corresponding case with no packing (from $\approx 78\%$ to $\approx 84\%$). However, the use of ASB packing resulted in reduced γ_{CH_4} . The reason is not immediately obvious. It is speculated that this could be related to the fact that the actual gas velocity will become very high when CH₄ is used as fuel and that ASB packing have shown an increased risk for channeling.
- The improvement in fuel conversion becomes even more significant if it is considered as function of oxygen carrier mass, or pressure drop over bed.
- Overall, the RMSR packing was found to provide very significant improvement in fuel conversion both for CO and CH₄. It also has a void factor of 0.96, meaning that it should not influence factors such as solids throughflow or pressure drop greatly. Thus, the use of this sort of packing materials to improve the performance of CLC looks promising.

Author contributions (Credit author statement)

Nasrin Nemati: Methodology, Validation, Investigation, Data Curation, Writing - Original Draft, Visualization.

Magnus Rydén: Conceptualization, Methodology, Resources, Writing - Review & Editing, Supervision, Project administration, Funding acquisition.

Declaration of Competing Interest

The authors declare that they have no known competing financial interests or personal relationships that could have appeared to influence the work reported in this paper.

Acknowledgement

This work has been supported by the Swedish Energy Agency (project 46525-1 - The application of confined fluidization in energy conversion).

References

- [1] A. Lyngfelt, Chemical Looping Combustion, in: F. Scala (Ed.), Fluidized-Bed Technologies for Near-Zero Emission Combustion and Gasification, Woodhead Publishing Limited, 2013, pp. 895–930.
- [2] J.A. Adanez, A.; Garcia-Labiano, F.; Gayan, P.; Luis, F., Progress in Chemical-Looping Combustion and Reforming Technologies, Prog. Energy Combust. Sci. 38 (2012) 215–282.
- [3] M. Rydén, A. Lyngfelt, Using steam reforming to produce hydrogen with carbon dioxide capture by chemical-looping combustion, Int. J. Hydrog. Energy 31 (10) (2006) 1271–1283.

- [4] A. Abad, et al., Evaluation of different strategies to improve the efficiency of coal conversion in a 50 kWth Chemical Looping combustion unit, Fuel 271 (2020) 117514.
- [5] M.N. Khan, et al., Integration of chemical looping combustion for cost-effective CO₂ capture from state-of-the-art natural gas combined cycles, Energy Conversion and Management: X 7 (2020) 100044.
- [6] E. Karchniwy, et al., The effect of turbulence on mass transfer in solid fuel combustion: RANS model, Combustion and Flame 227 (2021) 65–78.
- [7] A. Lyngfelt, et al., 11,000 h of Chemical-Looping Combustion Operation—Where are we and where do we want to go? Int. J. Greenhouse Gas Control (2019) 38–56.
- [8] J. Adanez, et al., Chemical Looping Combustion of Solid Fuels, Prog. Energy Combust. Sci. 65 (2018) 6–66.
- [9] T. Mattisson, et al., Chemical-looping technologies using circulating fluidized bed systems: Status of development, Fuel Process. Technol. 172 (2018) 1–12.
- [10] T. Berdugo Vilches, et al., Experience of more than 1000h of operation with oxygen carriers and solid biomass at large scale, Appl. Energy 190 (2017) 1174–1183.
- [11] C. Eder, et al., Particle Mixing in Bubbling Fluidized Bed Reactors with Immersed Heat Exchangers and Continuous Particle Exchange, Ind. Eng. Chem. Res. 59 (44) (2020) 19736–19750.
- [12] R.F. Pachler, et al., Investigation of the fate of nitrogen in chemical looping combustion of gaseous fuels using two different oxygen carriers, Energy 195 (2020) 116926.
- [13] L. Zhou, et al., Process simulation of Chemical Looping Combustion using ASPEN plus for a mixture of biomass and coal with various oxygen carriers, Energy 195 (2020) 116955.
- [14] K.M. Merrett, K.J. Whitty, Conversion of coal in a Fluidized Bed Chemical Looping Combustion Reactor with and without Oxygen Uncoupling, Energy Fuel 33 (2) (2019) 1547–1555.
- [15] K. Mayer, et al., Evaluation of a new DCFB reactor system for chemical looping combustion of gaseous fuels, Appl. Energy 255 (2019) 113697.
- [16] J. Aronsson, et al., Improved Gas-Solid Mass Transfer in Fluidized Beds: Confined Fluidization in Chemical-Looping Combustion, Energy Fuel (2019) 4442–4453.
- [17] J.D.M. Gabor, J. W., Engineering Development of Fluid-Bed Fluoride Volatility Processes, ACE Research and Development Report, 1965.
- [18] J.P.V. Sutherland, H. Kubota, G.L. Osberg, The Effect of Packing on a Fluidized Bed, A.I.Ch.E. Journal (1963) 437–441.
- [19] E.O. Echigoya, L. G., Oxidation of Ethylene Using Silver Catalyst Coated Strips in an Inert Fluidized Bed, Can. J. Chem. Eng. (1960) 108–112.
- [20] A.E.O. McIlhinney, L. G., Silver Sprayed Cylindrical Mesh Packing in a Fluidized Bed, Can. J. Chem. Eng. (1964) 232–233.
- [21] T.O. Ishii, L. G., Effect of Packing on the Catalytic Isomerization of Cyclopropane in Fixed and Fluidized Beds, AIChE J. 11 (1965) 279–287.
- [22] R.J.Z. Farrell, N. E., Kinetics and Mass Transfer in a Fluidized Packed-Bed: Catalytic Hydrogenation of Ethylene, A.I.Ch.E. Journal 25 (1979) 447–455.
- [23] B.Z. Buczek, Confined Fluidization of Fines in Fixed Bed of Coarse Particles, Chem. Process. Eng. 37 (2016) 545–557.
- [24] G.V. Claus, P. LE Goff, Hydrodynamic Study of Gas and Solid Flow Through a Screen-Packing, Can. J. Chem. Eng. 54 (1976) 143–147.
- [25] A.G.J.P. van der Ham, W.P.M. van Swaaij, A Small-Scale Regularly Packed Circulating Fluidized Bed, part I: Hydrodynamics, Powder Technol. 79 (1993) 17–28.
- [26] J. Aronsson, D. Pallarès, M. Rydén, A. Lyngfelt, Increasing Gas–Solids Mass transfer in Fluidized Beds by Application of Confined Fluidization—A Feasibility Study, Appl. Sci. 9 (2019).
- [27] H. Leion, et al., The use of ilmenite as an oxygen carrier in chemical-looping combustion, Chem. Eng. Res. Des. 86 (9) (2008) 1017–1026.
- [28] D.M. Mei, A. Abad, L.F. Diego, F. de García-Labiano, P. Gayan, J. Adanez, H. Zhao, Evaluation of manganese minerals for chemical looping combustion, Energy Fuel 29 (2015) 6605–6615.
- [29] M.M. Azis, et al., On the evaluation of synthetic and natural ilmenite using syngas as fuel in chemical-looping combustion (CLC), Chem. Eng. Res. Des. 88 (11) (2010) 1505–1514.
- [30] M. Rydén, et al., Ilmenite with addition of NiO as oxygen carrier for chemical-looping combustion, Fuel 89 (11) (2010) 3523–3533.
- [31] J.C. Adánez, A. Abad, P. Gayán, L.F. de Diego, F. García-Labiano, Ilmenite Activation during Consecutive Redox Cycles in Chemical-Looping Combustion, Energy Fuel 24 (2010) 1402–1413.
- [32] P.R. Moldenhauer, T. Mattisson, A. Jamal, A. Lyngfelt, Chemical-Looping Combustion with Heavy Liquid Fuels in a 10 kW pilot Plant, Fuel Process. Technol. 156 (2017) 124–137.
- [33] V.R. Stenberg, T. Mattisson, A. Lyngfelt, Experimental Investigation of Oxygen Carrier Aided Combustion (OCAC) with Methane and PSA off-gas, Appl. Sci. 11 (210) (2021).
- [34] G. Donsi, G. Ferrari, B. Formisani, Expansion behaviour of confined fluidized beds of fine particles, Can. J. Chem. Eng. 67 (1989).
- [35] N. Nemati, P. Andersson, V. Stenberg, M. Rydén, Experimental Investigation of the Effect of Random Packings on Heat Transfer and Particle Segregation in Packed-Fluidized Bed, Ind. Eng. Chem. Res. 60 (2021) 10365–10375.
- [36] P. Andersson, Experimental Determination of Heat transfer Coefficient to Horizontal Tube Submerged in Packed-fluidized Bed, MSc Thesis, Department of Space, Earth and Environment, Chalmers University of Technology: Göteborg, Sweden, 2020.